MODELING OF MAGNETIC HYSTERESIS UNDER WEAK MAGNETIC FIELDS AND TRIAXIAL STRESS STATE

Mushnikov A.N., Kryucheva K. D.
Institute of Engineering Science, Ural Branch of the Russian Academy of Sciences, Ekaterinburg, Russian Federation.

mushnikov@imach.uran.ru

Abstract: *The magnetomechanical hysteresis models of Jiles-Atherton and its modifications by Sablik are extended to treat magnetic properties in the case of triaxial stress state. Unlike the previous version, it is focused on weak magnetic fields. Results of simulation are compared with experimental data.*

Keywords: MAGNETIC HYSTERESIS, BULK STRESS STATE

1. Introduction

The problem of a theoretical description of changes in the magnetization of ferromagnets in external magnetic fields and mechanical stresses is associated with the need to take into account its total free energy, which depend in a complex way on internal factors (internal and applied stresses, magnetic anisotropy, dislocations, non-equilibrium point defects and inclusions, phase composition). One of the popular mathematical models of magnetic hysteresis of ferromagnetic materials was developed by Jiles and Atherton [1] and then was supplemented by the other scientists. The Jiles-Atherton model (JA-model) has a higher computational performance compared with Preisach phenomenological model and the Stoner-Wolfart hysteresis model [2]. And taking into account modifications, important advantages of the JA-model are the connection with the actual physical parameters of the ferromagnetic material, the calculation of major and any minor hysteresis loops on the same model parameters, the simulation of materials with isotropic and anisotropic properties, the calculation of the effect of mechanical stresses on magnetization.

The hysteresis model for the triaxial (bulk) stress state [3] was based on modifications of the JA-model [4, 5]. However, it turned out to be insufficiently suitable for describing processes in weak magnetic fields.

In the present paper, we refine the model for better describing the magnetization in weak fields, nevertheless maintaining adequate calculations in strong fields.

2. Mathematical formulation

The ideal (but impractical) experiment include triaxial stretching a cube with measuring magnetic characteristics simultaneously. In this paper, the bulk stress state is achieved by combining such types of loading as uniaxial tension/compression, torsion, and internal pressure. Listed types of loadings separately maybe not typical for some structures. They must be considered as the possibility of creating a stress state with independent changes in all three main stresses. The mechanical formulation was described in detail in [6].

Specimens are affected by axial load F, torque T and internal pressure p.

Normal stresses are calculated as:

$$(1)\quad \sigma_z = \frac{F}{\pi\left(R_{out}^2 - R_{in}^2\right)},$$

where R_{in} – internal radius of specimen, R_{out} – outer radius of specimen.

The volume-averaged values of the tangential stresses are equal to:

$$(2)\quad \tau = \frac{\left(R_{out} + R_{in}\right)}{\pi\left(R_{out}^4 - R_{in}^4\right)} T.$$

Under the action of internal pressure, tensile circumferential stresses σ_r and compressive radial stresses σ_θ are occurring. Their values, as functions of radius r, can be written as:

$$(3)\quad \begin{cases} \sigma_r = \dfrac{R_{in}^2}{R_{out}^2 - R_{in}^2}\left(1 - \dfrac{R_{out}^2}{r^2}\right) p, \\ \sigma_\theta = \dfrac{R_{in}^2}{R_{out}^2 - R_{in}^2}\left(1 + \dfrac{R_{out}^2}{r^2}\right) p \end{cases}$$

In the general case, the stress tensor in a cylindrical coordinate system is defined as:

$$(4)\quad A = \begin{pmatrix} \sigma_r & 0 & 0 \\ 0 & \sigma_\theta & \tau \\ 0 & \tau & \sigma_z \end{pmatrix}.$$

By solving the characteristic equation, we find the values of the main stresses averaged over the volume:

$$(5)\quad \begin{cases} \sigma_{j_1} = \dfrac{1}{R_{out} - R_{in}} \displaystyle\int_{r=R_{in}}^{R_{out}} \sigma_r dr \\ \sigma_{j_2} = \dfrac{1}{R_{out} - R_{in}} \displaystyle\int_{r=R_{in}}^{R_{out}} \dfrac{\sigma_\theta + \sigma_z + \sqrt{\left(\sigma_\theta + \sigma_z\right)^2 + 4\left(\tau^2 - \sigma_\theta \sigma_z\right)}}{2} dr \\ \sigma_{j_3} = \dfrac{1}{R_{out} - R_{in}} \displaystyle\int_{r=R_{in}}^{R_{out}} \dfrac{\sigma_\theta + \sigma_z - \sqrt{\left(\sigma_\theta + \sigma_z\right)^2 + 4\left(\tau^2 - \sigma_\theta \sigma_z\right)}}{2} dr \end{cases},$$

where indexes j_1, j_2 and j_3 take values 1, 2, 3 from condition $\sigma_1 \geq \sigma_2 \geq \sigma_3$.

To determine the directions of the main stresses, found main stresses are alternately substituted into the system of equations:

$$(6)\quad \begin{cases} \left(A - E\sigma_j\right)\vec{n}_j = 0 \\ n_{rj}^2 + n_{\theta j}^2 + n_{zj}^2 = 1 \end{cases},$$

where $\vec{n}_j$ is a vector with components n_{rj}, $n_{\theta j}$ and n_{zj}, (k = 1..3), E is identity matrix. In this system of equations, three of the four equations are linearly independent. Thus, having solved three systems, we obtain direction cosines of the main stresses. The angles corresponding to them are denoted by ψ_j.

The JA-model is constructed in two steps: on the first, the anhysteretic magnetization is calculated, then the hysteresis is simulated using a system of differential equations, taking into account changes in the external magnetic field. Anhysteretic magnetization is a magnetization obtained by the simultaneous action of a constant field and an alternating field with an amplitude decreasing to zero. Often, a modified Langevin function is used to describe the anhysteretic magnetization of isotropic materials:

$$(7)\quad M_{an} = M_s \left[\coth\left(\frac{H_e}{a}\right) - \frac{a}{H_e} \right].$$

But it has a singularity at $H_e = 0$ and therefore is not well suited for weak magnetic fields. To find a better function, we carried out an experiment to measure the anhysteretic magnetization curve of structural chromium-nickel steel 15KhN4D.

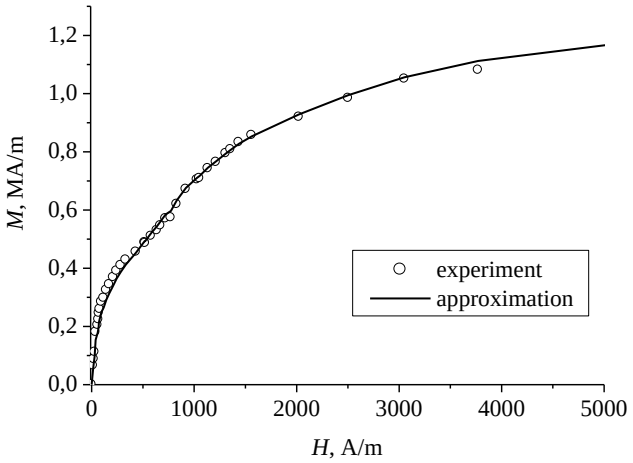

Fig. 1 *Anhysteretic magnetization curve and its approximation.*

This made it possible to choose a more suitable function that describes anhysteretic magnetization in weak magnetic fields with sufficient accuracy, and at the same time leads it to M_s when $H \to \infty$:

$$(8)\quad M_{an} = \frac{2}{\pi} M_s \arctan\left(\frac{H_e}{a}\right)$$

M_{an} is a function of effective field H_e:

$$(9)\quad H_e = H\cos\beta + \alpha M + H_\sigma,$$

where β is an angle between the direction of the external field and the vector of the resulting magnetization.

The basic equation of the JA-model, describing the change in total magnetization *M*, without separating it into reversible and irreversible components can be written as:

$$(10)\quad \frac{dM}{dH} = \frac{c}{1+c}\frac{dM_{an}}{dH} + \frac{1}{1+c}\frac{M_{an}(H) - M(H)}{\delta k - \alpha\left(M_{an}(H) - M(H)\right)}.$$

Magnetoelastic energy under the action of three orthogonal mechanical stresses consists of three independent parts. The formula proposed previously [3] significantly increases the complexity of calculations because it includes a derivative of magnetostriction which depending on the *M*. So, as the first approximation for weak fields, we use the more simple form:

$$(11)\quad H_\sigma = \sum_{j=1}^{3}\left[\left(b_{j1} + b_{j2}\sigma_j\right)\frac{M_{an}(H)}{M_s}\left(\cos^2\varphi_j - \upsilon\sin^2\varphi_j\right)\right].$$

Angles φ_j are solutions of three equations:

$$(12)\qquad \frac{d}{d\varphi_j}\left[\frac{1}{2}\alpha\mu_0 M^2 - \mu_0 HM\cos\left(\arccos n_{zj} - \varphi_j\right)\right] = 0$$

for *j* =1..3.

The angle β between the direction of the external field and the magnetization vector, which is necessary to calculate the effective field (9), can be expressed in terms of the angles that were found above.

$$(13)\quad n_r^* = \sum_{j=1}^{3}\cos\left(\frac{\varphi_j}{\psi_j}\arccos\left(n_{rj}\right)\right)$$

$$(14)\quad n_\theta^* = \sum_{j=1}^{3}\cos\left(\frac{\varphi_j}{\psi_j}\arccos\left(n_{\theta j}\right)\right)$$

$$(15)\quad n_z^* = \sum_{j=1}^{3}\cos\left(\psi_j - \varphi_j\right)$$

Then angle β is determined by the expression:

$$(16)\quad \beta = \frac{1}{\left|n^*\right|}\arccos n_z^*,$$

where $\left|n^*\right| = \sqrt{\left(n_r^*\right)^2 + \left(n_\theta^*\right)^2 + \left(n_z^*\right)^2}$. And also we take into account that $\cos\psi_j = n_{zj}$ are known values calculated by (6).

3. Results and discussion

Thus, the simulation of magnetic hysteresis in the bulk stress state must be performed in the following steps:

1. Calculating main stresses (5) and their directions (6).

2. Choosing range of *H* and the increment *dH*.

3. Solving the differential equation (10) at each step of *H*. Considering that anhysteretic magnetization is defined by equation (8), where effective field is given by expressions (9) and (11); angles between the magnetization vector and the directions of action of the main stresses (φ_1, φ_2 and φ_3) are the solutions of the system of three equations (12); the angle β between the magnetization vector and the direction of external magnetic field is defined by the formula (16).

Experimental studies were conducted on the hollow cylindrical and continuous flat specimens of structural steel 15KhN4D Permeameter magnetic measurements were made under applied loading. The tests were performed in the elastic strain region. A magnetic field was applied along the axis of the sample.

Although all the parameters of the JA-model have a physical meaning, their experimental determination is not a trivial problem. More practical are the methods of selecting the values of parameters which give a hysteresis loop, with sufficient accuracy reproducing the loop obtained in the experiment. M_s was directly obtained from the experimental major magnetic hysteresis loop. The difference between absolute saturation and the state of technical saturation (in a field of 60 kA/m) can be considered insignificant. To find the optimal parameters, the residuals *R* are minimized over all unknowns:

$$(17)\quad R = \sum_{i=1}^{n}\left(M_i^{\exp} - M(H_i)\right)^2,$$

where $\left(H_i, M_i^{\exp}\right)$ are experimental points "field-magnetization", *n* is a number of points in all hysteresis loops. For each set of parameters and for each point, the values $M(H_i)$ are calculated according to the mathematical model described in the previous section.

Analysis of the obtained loops with different stress variations showed that use of parameters *b* in (11) is not enough. Improving the fit between the experimental and calculated hysteresis loops was received by modifying the parameter *k*, which was previously considered as a constant:

$$(18)\quad k_\sigma = \left(\xi + (1-\xi)\exp\left(-\frac{\sigma}{\varsigma}\right)\right)k,$$

where ξ and ς are additional constants for material.

As examples, Figure 2 shows some series of calculated and experimental minor hysteresis loops of the investigated steel. The difference between experimental and calculated values does not

exceed 15%. Figure 2*a* represents hysteresis loops (only the first quadrant) at various values of the maximum magnetic field. Magnetic fields that are close to the geomagnetic field almost do not create irreversible part of magnetization.

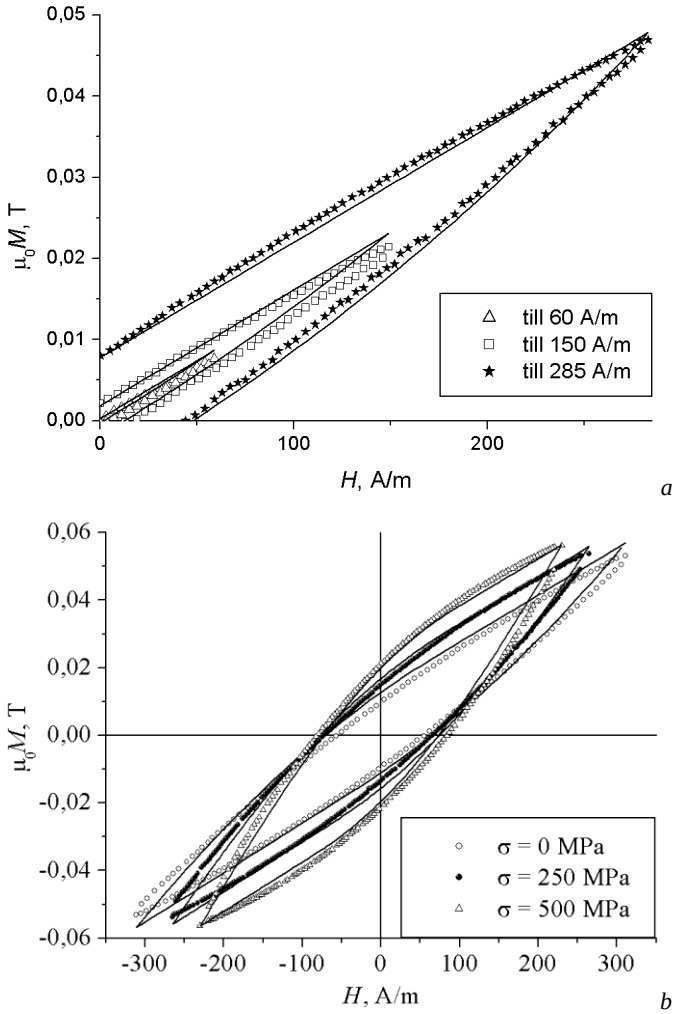

Fig. 2 *Comparison of mathematical model and experimentally obtained minor loops. Points from experiments; lines are the model.*

Figure 2*b* shows the effect of mechanical stresses on minor hysteresis loops obtained under magnetization up to the maximum induction of 0.05 T. Tensile stresses lead to the formation of a magnetic texture facilitating magnetization along the specimen axis. The minor loops measured in weak fields grow wider with increasing tensile stresses, their initial portion being steeper.

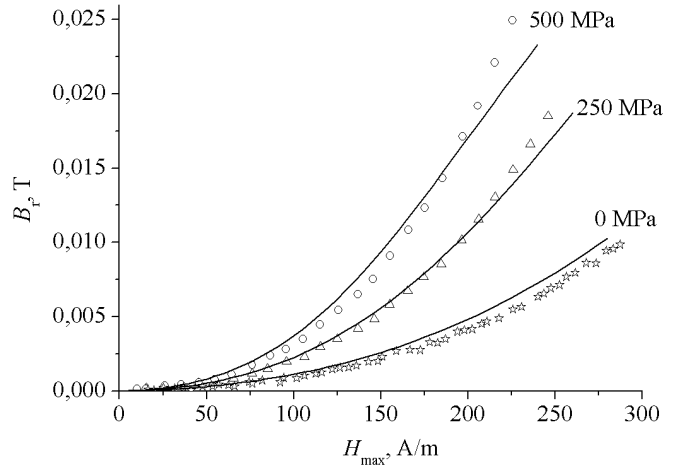

Fig. 3 *Residual induction as a function of mechanical stresses and the maximum value of the external magnetic field.*

A slight increase in coercive force is also observed. So in a magnetic field of a given strength, growing tensile stress is accompanied by an increase in the relative magnetized volume of the ferromagnetic material.

In details, figure 3 represents changes of residual induction B_r for various minor loops under mechanical stresses. The experiment was carried out on samples of the same grade of steel but from another melting. For this reason, the difference in the integral magnetic characteristics, which are calculated from major hysteresis loops, reaches 10%. In spite of this, for weak magnetic fields, the model rather accurately describes changes of the residual magnetization at the same parameters.

4. Conclusion

A modification of the mathematical model of hysteresis of Jiles-Atherton was proposed for the case of a bulk stress state and weak magnetic fields. It also includes some simplification for increase calculation speed. Comparison of calculated results with experimental data of structural steel showed the adequacy of the model.

5. Acknowledgements

The research was done within the state assignment, theme No. 0391-2016-0005. The experiments were carried out with the use of the equipment of the Plastometriya collective use center affiliated to IES UB RAS.

6. References

1. Jiles D. C., Atherton D. L. Theory of ferromagnetic hysteresis // Journal of Applied Physics, 1984, Vol. 55, p. 2115-2120.

2. Liorzou F., Phelps B., Atherton D. L. Macroscopic Models of Magnetization // IEEE Transactions on Magnetics, 2000, Vol. 36, №. 2, p. 418-428.

3. Mushnikov A.N., Putilova E.A. Mathematical Model of Magnetic Hysteresis Under Triaxial Stress State // MATHMODEL'17 Proceedings, p. 55-58.

4. Sablik M.J., Rubin S.W., Riley L.A., Jiles D.C., Kaminski D.A., Biner S.B. A model for hysteretic magnetic properties under the application of noncoaxial stress and field. - Journal of Applied Physics, 1993, v. 74, №1, p. 480-488.

5. Sablik M.J., Riley L.A., Burkhardt G.L., Kwun H., Cannell P.Y., Watts K.T., Langman R.A. Micromagnetic model for biaxial stress effects on magnetic properties. - Journal of Magnetism and Magnetic Materials, 1994, v. 132, №1-3, p. 131-148.

6. Gorkunov E.S., Zadvorkin S.M., Mushnikov A.N., Smirnov S.V., Yakushenko E.I. Effect of Mechanical Stresses on the Magnetic Characteristics of Pipe Steel // Journal of Applied Mechanics and Technical Physics, 2014, Vol. 3, p. 530-538.